Fuel Cells

DOI: 10.1002/anie.201102064

Oxygen Defects and Novel Transport Mechanisms in Apatite Ionic Conductors: Combined ^{17}O NMR and Modeling Studies**

Pooja M. Panchmatia, Alodia Orera, Gregory J. Rees, Mark E. Smith, John V. Hanna, Peter R. Slater,* and M. Saiful Islam**

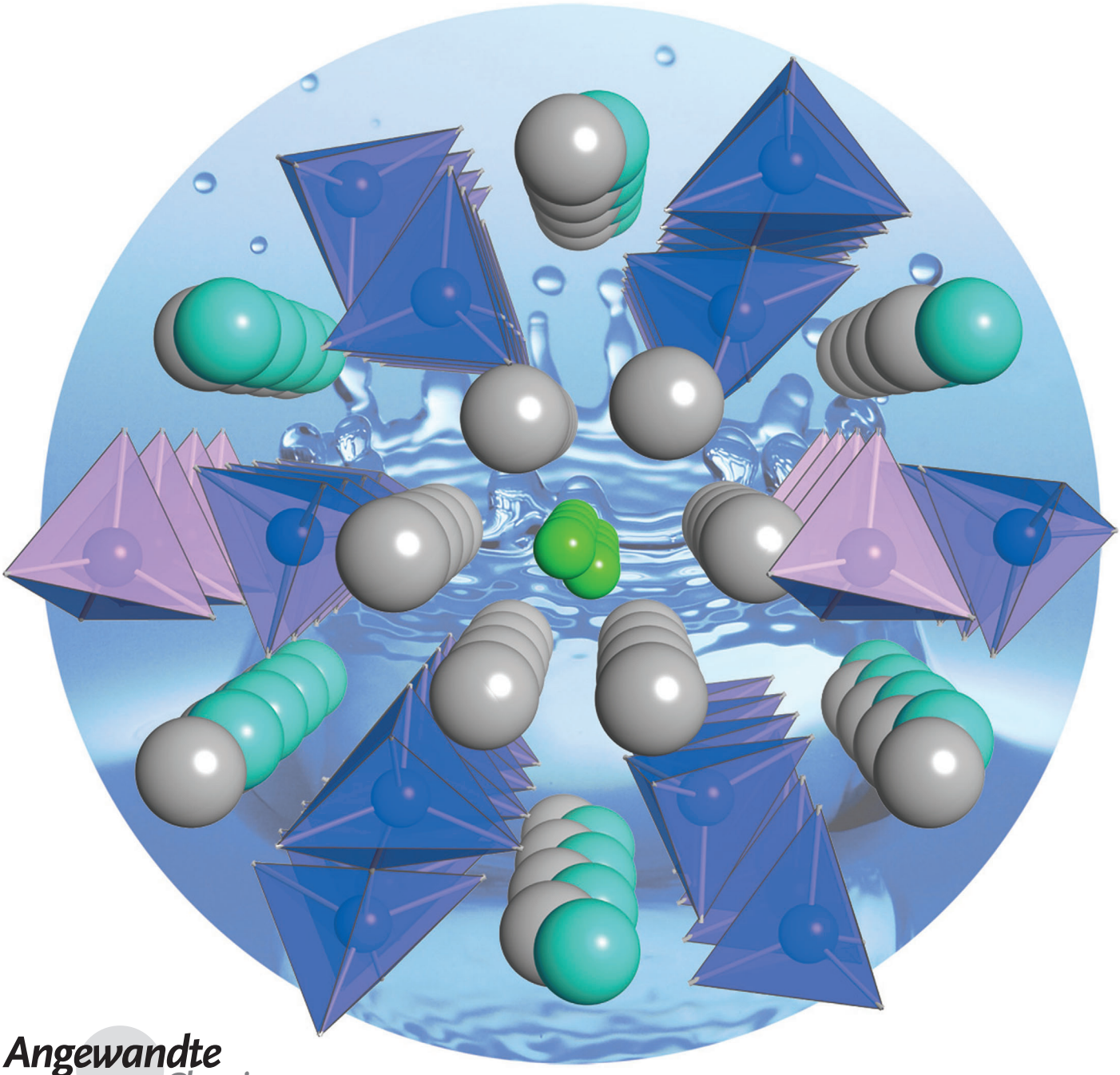

The viability of low carbon energy technologies such as fuel cells is crucially dependent on the fundamental advances in the component materials.[1–4] Si- and Ge-based apatite compounds are attracting considerable interest as new oxide-ion conducting electrolytes for use in solid oxide fuel cells. However, a complete understanding of their local structural and conduction properties on the atomic scale is still lacking. Here, we utilize a combined nuclear magnetic resonance (NMR) and computational approach to elucidate the defect sites and conduction mechanisms in the novel apatite compound $La_8Y_2Ge_6O_{27}$, which exhibits high oxide-ion conductivity and high oxygen excess. Through solid-state ^{17}O NMR and computer modeling studies we show that at ambient temperature the interstitial oxide-ion defects are associated with the Ge leading to the formation of five-coordinate Ge. In addition, we show that oxide-ion migration occurs through cooperative mechanisms involving the framework tetrahedra, with evidence of a novel substitution-mediated conduction mechanism, which facilitates oxide-ion transport despite the lack of open conduction pathways. The results are therefore of great significance in the search for new oxide-ion conductors for clean energy applications, as well as being of relevance to hydroxyapatite biomaterials.

Research on electrolytes for solid oxide fuel cells (SOFCs) has been dominated by oxide-ion vacancy conductors, in particular fluorite or perovskite-type oxides.[1–4] In these materials, the oxide-ion vacancies are introduced through acceptor doping, which then allows oxide-ion conduction by a conventional hopping mechanism through these vacancy defects.

Despite the intense research on these systems, there is still a need to develop new electrolytes with improved properties to allow operation of SOFCs at intermediate temperatures (500–700 °C). In this respect there has been interest in a range of new structure classes showing high oxide-ion conduction, including apatite-type silicates/germanates ($La_{9.33+x}(Si/Ge)_6O_{26+3x/2}$)[5–21] and melilite-type $La_{1+x}Sr_{1-x}Ga_3O_{7+x/2}$.[22] An unusual feature of these systems is that rather than oxide-ion vacancies being the conducting defects (as for conventional fluorite and perovskite oxides), the conduction is mediated by oxide ions located at interstitial sites. The clear demarcation between interstitial ion conduction and conventional vacancy conduction is emphasized by the fact that the introduction of oxide-ion vacancies leads to lower rather than higher conductivity in the apatite materials.[5]

The importance of interstitial oxide ions, however, has made an understanding of the conduction mechanisms in apatite materials difficult, since such defects are difficult to locate precisely; they also lead to local distortions as indicated by modelling studies,[13,16,19] and indirectly through the observation of large atomic displacement parameters for the oxygen sites in neutron diffraction studies.[7–9,14,17,18] Indeed, the actual location of the interstitial site in the apatite systems has attracted significant controversy.[5,13–20]

These apatite materials have the general formula, $A_{10-x}(Si/Ge)_6O_{26+y}$ (A = rare earth/alkaline earth), and their structures may be considered as composed of an $A_{4-x}(Si/GeO_4)_6$ framework, with the remaining A_6O_2 units occupying the channels within this framework. The oxide-ion excess (y) has been reported to be either between the oxygen sites at the center of the channels, or associated with the framework.[5,7,13–20] One reason for these literature discrepancies is the large local distortions around the interstitial site, making determinations from diffraction studies difficult, as these focus on the long-range average structure.

Herein, we present a comprehensive examination of the location of the interstitial oxide-ion defects in apatite germanates using techniques that provide a more local, element specific probe to reveal environments on the atomic scale. In particular we utilize a powerful approach where atomistic simulation and density functional theory (DFT) techniques are combined with ^{17}O solid-state NMR studies, which are the first of such NMR data acquired on these apatite systems.

The key composition examined was $La_8Y_2Ge_6O_{27}$ as it contains high oxide-ion excess and shows high oxide-ion conductivity. Room-temperature cell parameters and atomic positions obtained for $La_8Y_2Ge_6O_{27}$ from the Rietveld refinement of diffraction data[17] were used to develop an atomistic potential model, and provided the starting point for the DFT-based calculations. The results indicated that the complex structure was reproduced by the computational methods, showing good agreement with the experimental data (see Table S-1 in the Supporting Information).

For $La_8Y_2Ge_6O_{27}$, the location of the interstitial oxide-ion site was first analyzed by DFT calculations. In the optimized structures the incorporation of interstitial oxide ions (O5) occurs preferentially between two GeO_4 tetrahedra causing local relaxation of the tetrahedra (Figure 1). In the relaxed structure, the O5 interstitial is closer to one Ge (with a Ge–O distance of 1.99 Å). Hence the DFT calculations suggest that on introduction of interstitial oxide ions the resulting species is a GeO_5 unit. This is in line with neutron diffraction studies,[7] and recent local structure studies using pair distribution function analysis[15] of related Ge-based apatite compounds.

To provide experimental confirmation for the interstitial site, ^{17}O NMR data were collected for ^{17}O-enriched $La_8Y_2Ge_6O_{27}$. For comparison, data were also collected for the samples $La_8YCaGe_6O_{26.5}$ and $La_{7.5}Ca_{2.5}Ge_6O_{25.75}$: the former contains half the interstitial oxide-ion content com-

[*] Dr. P. M. Panchmatia, Prof. M. S. Islam
Department of Chemistry, University of Bath
Bath, BA2 7AY (UK)
E-mail: m.s.islam@bath.ac.uk
Dr. A. Orera, Dr. P. R. Slater
School of Chemistry, University of Birmingham
Birmingham, B15 2TT (UK)
E-mail: p.r.slater@bham.ac.uk
G. J. Rees, Prof. M. E. Smith, Dr. J. V. Hanna
Department of Physics, University of Warwick
Coventry, CV4 7AL (UK)
E-mail: j.v.hanna@warwick.ac.uk

[**] This work was supported by the EPSRC and the European Regional Development Fund. The computations were run on the HECToR facilities through the Materials Chemistry Consortium.

Supporting information for this article is available on the WWW under http://dx.doi.org/10.1002/anie.201102064.

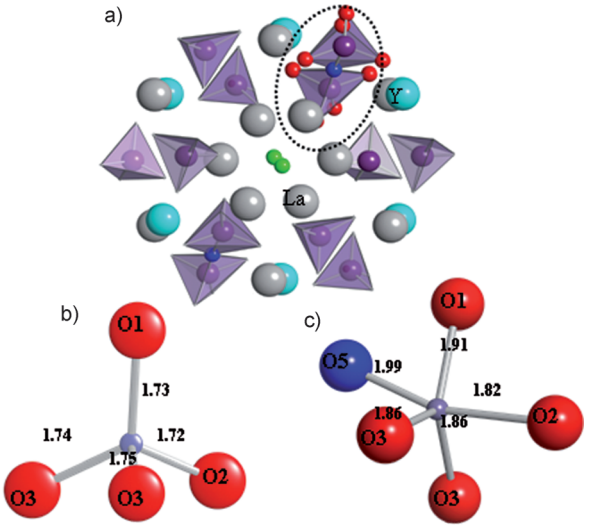

Figure 1. a) $La_8Y_2Ge_6O_{27}$ apatite framework showing GeO_4 tetrahedra, La/Y ions and two oxide-ion interstitials. b,c) Local structure and Ge–O distances of GeO_4 unit and an O5 interstitial forming a GeO_5 unit from DFT calculations: La (gray), Y (cyan), O1-3 tetrahedral (red), O4 channel (green), and O5 interstitial (dark blue).

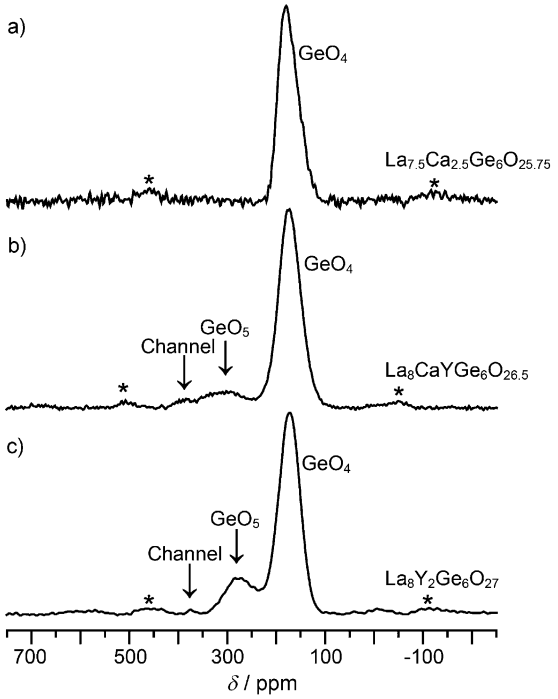

Figure 2. ^{17}O MAS NMR data at 54.22 MHz and assignments for a) $La_{7.5}Ca_{2.5}Ge_6O_{25.75}$, b) $La_8Y_2CaGe_6O_{26.5}$, and c) $La_8Y_2Ge_6O_{27}$. The asterisks denote the positions of spinning sidebands.

pared to $La_8Y_2Ge_6O_{27}$, while the latter contains no interstitial oxide ions, but rather oxide-ion vacancies. As a result of the lack of interstitial oxide ions in $La_{7.5}Ca_{2.5}Ge_6O_{25.75}$, the conductivity is very low (see Figure S1 in the Supporting Information). The ^{17}O enrichment strategy made use of the ability of these apatite germanates to incorporate water at temperatures $< 500\,^{\circ}C$.[9,11] The samples were therefore first treated hydrothermally in the presence of ^{17}O-enriched water, before subsequently heating at 700 °C in Ar to dry the sample and ensure that equilibration had occurred.

The ^{17}O nucleus has been demonstrated to be a very good probe of the local structure of oxide materials because of its large chemical shift range.[23–27] Despite the quadrupolar nature of this nucleus ($I = 5/2$, $Q = -25.6$ mb)[25,26] the overall size of the ^{17}O quadrupole interaction (and resultant quadrupole coupling constants (C_Q) see Table S2 and Figure S2 in the Supporting Information) in these materials is sufficiently small such that conventional magic angle spinning (MAS) alone can be applied for resolution enhancement. Indeed, high-resolution ^{17}O NMR spectroscopy has been used successfully to probe oxide-ion conductors such as $Bi_4V_2O_{11}$-based compounds.[27]

The ^{17}O MAS NMR data of Figure 2a show that a single resonance for $La_{7.5}Ca_{2.5}Ge_6O_{25.75}$ is observed at an apparent (uncorrected) chemical shift (δ) of around 170 ppm, consistent with oxide ions within a GeO_4 unit. In contrast, the spectra for $La_8YCaGe_6O_{26.5}$ and $La_8Y_2Ge_6O_{27}$ (Figure 2b,c, respectively) demonstrated the presence of additional downfield resonances at apparent chemical shifts around 280 and 370 ppm. The intensity increase of the resonance at a δ around 280 ppm in going from $La_8YCaGe_6O_{26.5}$ to $La_8Y_2Ge_6O_{27}$ suggests that this resonance represents the presence of increasing interstitial oxide ions. However, the relative intensity of this resonance appears too large to be associated simply with isolated interstitial oxide ions. As noted, the DFT modeling data from these systems proposes the formation of an overall GeO_5 unit (Figure 1c) rather than isolated interstitial oxide ions being loosely associated with GeO_4 tetrahedra.

To support this assignment, the expected longer Ge–O bond lengths for the GeO_5 moiety (in comparison to the predominant GeO_4 counterparts) would induce increased ionic character to the oxide bonding and thus result in a small downfield shift from the increased deshielding. From this new description the nominal stoichiometric formulae $La_8YCaGe_6O_{26.5}$ and $La_8Y_2Ge_6O_{27}$ can be rewritten as $La_8YCa(GeO_4)_{5.5}(GeO_5)_{0.5}O_2$ and $La_8Y_2(GeO_4)_5(GeO_5)O_2$, respectively, which thus yield relative ratios for oxygen sites associated with (GeO_5) units to (GeO_4) units equal to 1:9 and 1:5 respectively, for these systems. From the two predominant ^{17}O MAS NMR resonances in Figure 2a,b ratios of the chemical shift δ at around 280 ppm to the δ at around 170 ppm of around 1:9 and 1:4 are measured, which are in good agreement with these new descriptions.

In both the $La_8YCaGe_6O_{26.5}$ and $La_8Y_2Ge_6O_{27}$ samples, the third weak downfield resonance at a δ around 370 ppm is attributed to the channel oxide-ion site, which is not observed at all for $La_{7.5}Ca_{2.5}Ge_6O_{25.75}$. This assignment is strongly correlated with the much longer metal (La)–O bond lengths characterizing the channel oxide ions[17] and a larger downfield shift is expected. The observed absence of this resonance for the $La_{7.5}Ca_{2.5}Ge_6O_{25.75}$ sample is most likely related to the poor oxide-ion conductivity of this latter phase meaning that equilibration in the ^{17}O exchange process was incomplete.

To analyze further the ^{17}O MAS NMR assignments, DFT calculations were performed to predict the ^{17}O chemical shifts

expected for the $La_8Y_2Ge_6O_{27}$ system. The calculated total ^{17}O solid-state NMR spectrum is shown in Figure 3, which is created from a summation of the 27 individual ^{17}O chemical shifts from the oxide-ion positions comprising the unit cell. These calculations clearly corroborate the position of the channel (downfield) and bulk GeO_4 framework species

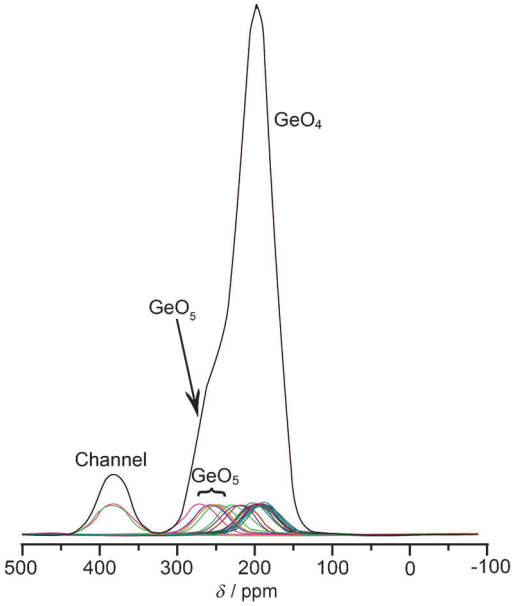

Figure 3. Simulated ^{17}O NMR spectrum for $La_8Y_2Ge_6O_{27}$ from DFT calculations. The scaling of the ^{17}O chemical shifts was undertaken at both the low-field (channel oxygen) and high-field (framework GeO_4) ends to facilitate comparison with the measured data (Figure 2). The calculations predict the small shift separation between the GeO_5 units (interstitial induced) and framework GeO_4 tetrahedra.

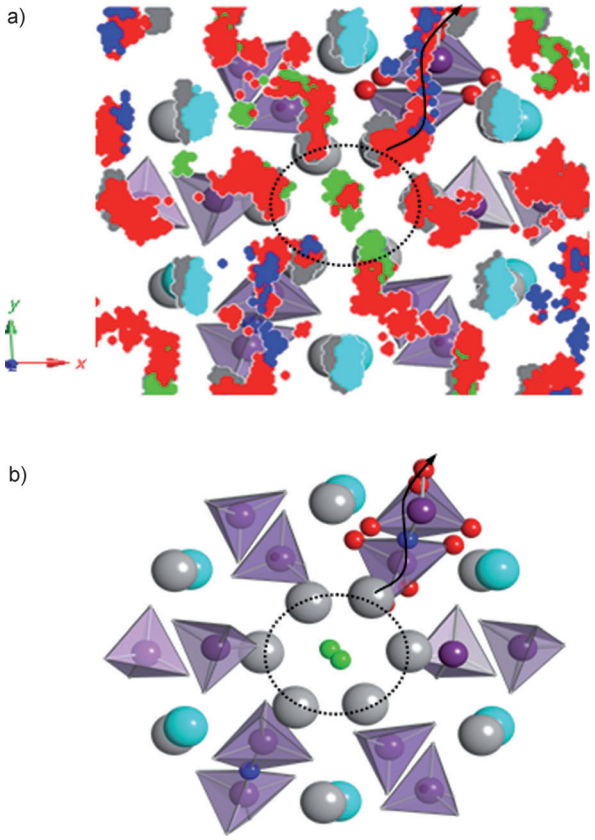

Figure 4. Oxygen diffusion in the *ab* plane of $La_8Y_2Ge_6O_{27}$ from MD simulations. a) Ion trajectories showing the conduction pathway (arrow) and oxygen Frenkel formation (green). b) Schematic representation of the corresponding structure highlighting the pathway between channels: La (gray), Y (cyan), O tetrahedral (red), O channel (green), O interstitial (blue), and dashed circles indicate the channel area.

(upfield). More importantly, the calculations are also sensitive enough to predict the small shift separation between the GeO_5 units (interstitial induced) and framework GeO_4 tetrahedra. Relative to a fixed internal standard aligning the calculated and experimental ^{17}O MAS NMR spectra, the agreement between the calculated and experimental apparent shift positions (δ) is within ± 50 ppm.

With the experimental confirmation of the interstitial oxide-ion site being associated with the Ge at ambient temperature leading to five coordinate Ge, the modeling work was then extended to molecular dynamics (MD) simulations to probe the mechanism of oxide-ion diffusion at the atomic scale and elevated temperatures, which is difficult to extract from experiment alone.

The results from the MD study of $La_8Y_2Ge_6O_{27}$ over long simulation time scales suggest a range of conduction pathways, with evidence for conduction along the *c* direction, as well as perpendicular to the channels (Figure 4), the latter allowing interstitial oxide ions to pass between channels. The diffuse distribution and overlapping of different oxygen positions shown in Figure 4 indicates that numerous oxide ions are moving between lattice and interstitial sites. The plots of mean square displacements (see Figure S3 in the Supporting Information) also indicate that all oxide ions are mobile.

Detailed analysis of the simulated trajectories suggests a novel substitution-mediated mechanism for oxide-ion diffusion between channels. Figure 5 shows simulation snapshots of two adjacent Ge/O units with corresponding changes in local Ge–O separations listed in Table 1. The mechanism is reminiscent of S_N2 (nucleophilic substitution) reactions which are common in organic chemistry. In this case, an oxide interstitial "attacks" the Ge forming a bond with it and leading to another oxide ion "departing" the same Ge unit

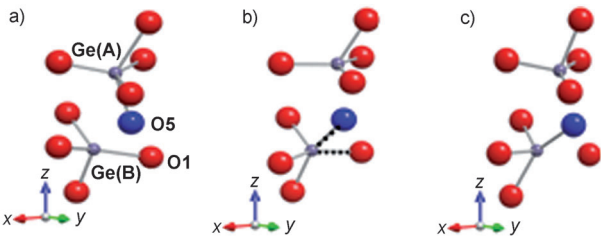

Figure 5. Sequence of MD simulation snapshots indicating the proposed interstitial conduction mechanism. a) Two adjacent Ge units and oxide-ion interstitial O5 (blue). b) O5 interstitial "attacking" the Ge of the Ge(B) tetrahedron in an intermediate state. c) O5 forming a bond with Ge(B) leading to the "freeing" of another oxide ion O1.

Table 1: Ge–O separations corresponding to the MD simulation snapshots shown in Figure 5.

Ion pair[a]	a)	b)	c)
Ge(A)–O5 [Å]	1.94	2.13	2.10
Ge(B)–O1 [Å]	1.96	1.97	2.16
Ge(B)–O5 [Å]	2.05	1.90	1.75

[a] Equilibrium bonds in tetrahedron Ge–O(1,2,3) around 1.75 Å.

into an adjacent channel; this occurs through a concerted substitution mechanism and can be termed "S_N2-like" interstitial conduction. Such processes will occur rapidly at elevated temperatures, where oxide-ion conduction becomes significant. So under these elevated temperature conditions, the five-coordinate Ge may now become a transient intermediate species for the conduction process. Evidence in support of this process comes from recent Raman spectroscopy studies of other oxygen-excess Ge-based apatites,[10] in which a new band was observed and attributed to five-coordinate Ge; the intensity of this band decreases on increasing the temperature, related to freeing of the interstitial oxide ion from the GeO_5 unit.

Such a mechanism was only postulated in our earlier work,[16] whereas the studies here have elucidated this process. Furthermore, the ^{17}O MAS NMR results provide the first experimental evidence in support of substitution mechanisms, involving the GeO_4 tetrahedra. The NMR data show high ^{17}O enrichment of only those oxide ions that are attached to Ge, with low enrichment for the channel oxide-ion sites. A non-uniform enrichment motif such as that observed experimentally in Figure 2 (where there is higher enrichment of oxygen sites connected to Ge, compared to the channel oxygen sites) can only be explained by substitution processes involving the GeO_4 units.

It is possible that such transport mechanisms are occurring in other ionic conductors containing tetrahedral moieties, particularly if the systems accommodate interstitial oxide ions, for example, melilite-type $La_{1+x}Sr_{1-x}Ga_3O_{7+x/2}$.[22] A key feature for such oxide-ion conduction is the intrinsic flexibility and dynamical deformation of the tetrahedra in these structures, as shown in recent MD studies of the melilite system.[28]

In addition to ion conduction in the *ab* plane, the results suggest that conduction in the *c* direction can occur through pathways down the center of adjacent tetrahedra (see Figure S4 in the Supporting Information). Another interesting point is that, contrary to earlier predictions, conduction in these apatites is anisotropic involving a direct pathway of the channel (O4) oxide ions along the *c* direction.[6] The results here indicate no evidence for any significant conduction through this route. Rather the main conduction pathway for the O4 oxide ions is in the *ab* plane leading to the creation of Frenkel-type defects, and subsequent conduction of the interstitial oxide ions through the described mechanisms. Such oxygen Frenkel creation is shown in Figure 4 in which the channel oxygens migrate into interstitial positions.

The oxide-ion diffusion coefficient (D) can be derived using the mean square displacements from MD data. The oxide-ion conductivity was then estimated using the standard Nernst–Einstein relation, $\sigma = DNq^2/fTk_B$. As the Haven ratio (f) is not known for the apatite structure, values for other fast-ion conductors[29] have been used to generate an estimated conductivity range of $0.8–1.3 \times 10^{-2}$ S cm^{-1} at 1073 K. This is in good agreement with the experimental conductivity (around 1.0×10^{-2} S cm^{-1}) for $La_8Y_2Ge_6O_{27}$ (see Figure S1 in the Supporting Information),[17] and hence provides further evidence for the validity of the modeling approach.

In summary, combined ^{17}O MAS NMR, molecular dynamics, and DFT studies of apatite fast-ion conductors show that the interstitial oxide ions lie within the bonding sphere of Ge leading to five-coordinate Ge at ambient temperature. At elevated temperatures, where oxide-ion conduction becomes significant, the modeling work indicates the importance of the GeO_4 units in the conduction process, which is supported experimentally by the ready ^{17}O enrichment of the GeO_4 tetrahedra. A novel "S_N2-like" interstitial mechanism is indicated, which allows oxide-ion conduction to occur between channels in the *ab* plane despite the lack of an apparent open pathway. We suggest that such processes may occur in other interstitial oxide-ion conductors comprised of tetrahedral units because of the ability of the tetrahedral cation to increase its coordination sphere. These results are therefore of great significance in the search for new ionic conductors for solid oxide fuel cells and other clean energy applications.

Experimental Section

Extended details can be found in the Supporting Information.

Experiments: Samples of $La_{7.5}Ca_{2.5}Ge_6O_{25.75}$, $La_8YCaGe_6O_{26.5}$, and $La_8Y_2Ge_6O_{27}$ were prepared using standard solid-state reactions heated to 1100 °C. Phase purity was confirmed through X-ray powder diffraction (Bruker D8 diffractometer with Cu $K_{\alpha 1}$ radiation). ^{17}O isotopic enrichment was achieved using 90 % ^{17}O-enriched water, under hydrothermal conditions and subsequent dehydration at 700 °C under Ar. Variable B_0 field solid-state ^{17}O magic angle spinning (MAS) NMR spectra were acquired at five Larmor frequencies in the range from 40.68 to 108.49 MHz. All data was acquired using rotor synchronized MAS spin echo (θ–τ–2θ–τ) experiments.

Computations: Molecular dynamics (MD) simulations used the DLPOLY code[30] with shell-model ionic potentials, and were carried out at higher temperatures than the NMR experiments, which allowed for high-quality statistics from long simulation timescales. DFT calculations used the VASP[31] code for the geometry optimizations, and the GIPAW-based NMR-CASTEP[32] code for the electric field gradient and isotropic shift calculations. VESTA[33] was used for analysis of the results. The methods used here have been applied successfully to fuel cell materials[16,28,34] and other related oxides.[35]

Received: March 23, 2011
Revised: June 28, 2011
Published online: August 24, 2011

Keywords: computer simulations · fuel cells · NMR spectroscopy · solid-state structures

[1] J. B. Goodenough, *Annu. Rev. Mater. Res.* **2003**, *33*, 9.
[2] S. M. Haile, *Acta Mater.* **2003**, *51*, 5981.

[3] a) L. Malavasi, C. A. J. Fisher, M. S. Islam, *Chem. Soc. Rev.* **2010**, *39*, 4370; b) A. J. Jacobson, *Chem. Mater.* **2010**, *22*, 660.
[4] A. Orera, P. R. Slater, *Chem. Mater.* **2010**, *22*, 675.
[5] E. Kendrick, M. S. Islam, P. R. Slater, *J. Mater. Chem.* **2007**, *17*, 3104.
[6] a) S. Nakayama, H. Aono, Y. Sadaoka, *Chem. Lett.* **1995**, 431; b) S. Nakayama, M. Sakamoto, M. Higuchi, K. Kodaira, M. Sato, S. Kakita, T. Suzuki, K. Itoh, *J. Eur. Ceram. Soc.* **1999**, *19*, 507.
[7] S. S. Pramana, W. T. Klooster, T. J. White, *Acta Crystallogr. Sect. B* **2007**, *63*, 597.
[8] J. E. H. Sansom, D. Richings, P. R. Slater, *Solid State Ionics* **2001**, *139*, 205.
[9] a) L. Leon-Reina, J. M. Porras-Vasquez, E. R. Losilla, M. A. G. Aranda, *J. Solid State Chem.* **2007**, *180*, 1250; b) D. Marrero-Lopez, M. C. Martin-Sedeno, J. Pena-Martinez, J. C. Ruiz-Morales, P. Nunez, M. A. G. Aranda, J. R. Ramos-Barrado, *J. Power Sources* **2010**, *195*, 2496.
[10] A. Orera, M. Sanjuan, E. Kendrick, V. Orera, P. R. Slater, *J. Mater. Chem.* **2010**, *20*, 2170.
[11] A. Orera, P. R. Slater, *Solid State Ionics* **2010**, *181*, 110.
[12] S. S. Pramana, W. T. Klooster, T. J. White, *J. Solid State Chem.* **2008** *181*, 1717.
[13] a) J. R. Tolchard, M. S. Islam, P. R. Slater, *J. Mater. Chem.* **2003**, *13*, 1956; b) A. Jones, P. R. Slater, M. S. Islam, *Chem. Mater.* **2008**, *20*, 5055.
[14] R. Ali, M. Yashima, Y. Matsushita, H. Yoshioka, K. Okoyama, F. Izumi, *Chem. Mater.* **2008**, *20*, 5203.
[15] L. Malavasi, A. Orera, P. R. Slater, P. M. Panchmatia, M. S. Islam, J. Siewenie, *Chem. Commun.* **2011**, *47*, 250.
[16] E. Kendrick, M. S. Islam, P. R. Slater, *Chem. Commun.* **2008**, 715.
[17] E. Kendrick, A. Orera, P. R. Slater, *J. Mater. Chem.* **2009**, *19*, 7955.
[18] S. Guillot, S. Beaudet-Savignat, S. Lambert, R. N. Vannier, P. Rousse, F. Porcher, *J. Solid State Chem.* **2009** *182*, 3358.
[19] E. Bechade, O. Masson, T. Iwata, I. Julien, K. Fukuda, P. Thomas, E. Champion, *Chem. Mater.* **2009**, *21*, 2508.
[20] P. M. Panchmatia, A. Orera, E. Kendrick, J. V. Hanna, M. E. Smith, P. R. Slater, M. S. Islam, *J. Mater. Chem.* **2010**, *20*, 2766.
[21] a) Y. Kim, D. K. Shin, E. C. Shin, H. H. Seo, J. S. Lee, *J. Mater. Chem.* **2011**, *21*, 2940; b) T. Liao, T. Sasaki, S. Suehara, Z. Sun, *J. Mater. Chem.* **2011**, *21*, 3234; c) Y. Ohnishi, A. Mineshige, Y. Daiko, M. Kobune, H. Yoshioka, T. Yazawa, *Solid State Ionics* **2010**, *181*, 1697.
[22] X. Kuang, M. A. Green, H. Niu, P. Zajdel, C. Dickinson, J. B. Claridge, L. Jantsky, M. J. Rosseinsky, *Nat. Mater.* **2008**, *7*, 498.
[23] B. O. Skadtchenko, Y. X. Rao, T. F. Kemp, P. Bhattacharya, P. A. Thomas, M. Trudeau, M. E. Smith, D. M. Antonelli, *Angew. Chem.* **2007**, *119*, 2689; *Angew. Chem. Int. Ed.* **2007**, *46*, 2635.
[24] S. E. Ashbrook, M. E. Smith, *Chem. Soc. Rev.* **2006**, *35*, 718.
[25] K. J. D. MacKenzie, M. E. Smith, "Multinuclear Solid State NMR of Inorganic Materials" Pergamon, Oxford, **2002**.
[26] M. E. Smith, E. R. H. van Eck, *Prog. Nucl. Magn. Reson. Spectrosc.* **1999**, *34*, 159.
[27] N. Kim, C. P. Grey, *Science* **2002**, *297*, 1317.
[28] C. Tealdi, P. Mustarelli, M. S. Islam, *Adv. Funct. Mater.* **2010**, *20*, 3874.
[29] G. E. Murch, *Solid State Ionics* **1982**, *7*, 177.
[30] W. Smith, C. W. Yong, P. M. Rodger, *Mol. Simul.* **2002**, *28*, 385.
[31] G. Kresse, J. Furthmüller, *Phys. Rev. B* **1996**, *54*, 11169.
[32] S. J. Clark, M. D. Segall, C. J. Pickard, P. J. Hasnip, M. J. Probert, K. Refson, M. C. Payne, *Z. Kristallogr.* **2005**, *220*, 567.
[33] K. Momma, F. Izumi, *J. Appl. Crystallogr.* **2008**, *41*, 653.
[34] a) E. Kendrick, J. Kendrick, K. S. Knight, M. S. Islam, P. R. Slater, *Nat. Mater.* **2007**, *6*, 871; b) A. Chroneos, D. Parfitt, J. A. Kilner, R. W. Grimes, *J. Mater. Chem.* **2010**, *20*, 266; c) M. S. Islam, *Philos. Trans. R. Soc. London Ser. A* **2010**, *368*, 3255.
[35] a) A. A. Sokol, A. Walsh, C. R. A. Catlow, *Chem. Phys. Lett.* **2010**, *492*, 44; b) N. H. de Leeuw, J. R. Bowe, J. A. L. Rabone, *Faraday Discuss.* **2007**, *134*, 195; c) A. R. Armstrong, C. Lyness, P. M. Panchmatia, M. S. Islam, P. G. Bruce, *Nat. Mater.* **2011**, *10*, 223; d) C. A. J. Fisher, M. S. Islam, *J. Mater. Chem.* **2008**, *18*, 1209.

